Journal of Solid State Chemistry **158,** 1–13 (2001)
doi:10.1006/jssc.2000.8976, available online at http://www.idealibrary.com on IDEAL®

The Crystal Structure and Vibrational Spectra of Mono-L-valinium Nitrate: DSC, FTIR, and X-ray Diffractional Study of Low-Temperature Phase Transition

Ivan Němec,[1] Ivana Císařová, and Zdeněk Mička

Department of Inorganic Chemistry, Faculty of Science, Charles University of Prague, Albertov 2030, 128 40 Prague 2, Czech Republic

Received May 30, 2000; in revised form August 14, 2000; accepted October 3, 2000; published online March 7, 2001

The X-ray structural analysis of two mono-L-valinium nitrate phases (293 and 130 K) has been carried out. In the both phases substance crystallizes in the monoclinic space group $P2_1$: phase I $a = 10.8369(3)$, $b = 18.4590(10)$, $c = 5.62190(2)$ Å, $\beta = 129.07(3)^\circ$, $V = 873.11(5)$ Å^3, $Z = 4$, $R = 0.0509$ for 1514 observed reflections, and phase II $a = 10.765(2)$, $b = 18.2290(10)$, $c = 11.109(2)$ Å, $\beta = 128.64(1)^\circ$, $V = 1702.7(5)$ Å, $Z = 8$, $R = 0.0257$ for 4316 observed reflections. The crystal structures are formed by L-valinium cations and nitrate anions connected by an extensive system of hydrogen bonds. Phase I is characterized by the presence of isopropyl groups structural disorder between two positions. Low-temperature phase II exhibits an increase of the unit cell volume, and absence of isopropyl groups disorder. The positions of nitrate groups remain practically unchanged in both the phases. The FTIR and FT Raman spectra of natural and deuterated compounds were recorded and interpreted. The FTIR spectra were studied down to a temperature of 90 K. DSC measurements were carried out in the temperature range 95–400 K. The order–disorder phase transition between the phases I and II was observed at ca. 250 K. © 2001 Academic Press

Key Words: **mono-L-valinium nitrate; crystal structure; vibrational spectra; phase transition; DSC measurement.**

INTRODUCTION

The family of amino acid addition compounds with inorganic oxyacids is interesting, among other things, in that some of its members exhibit unique physical properties (i.e., ferroelectric, pyroelectric, etc.). Probably the most important members of the group of hydrogen-bonded ferroelectrics are triglycine sulfate (TGS) (1) and diglycine nitrate (DGN) (2). A complex phase transition mechanism (3) between the ferroelectric and paraelectric phases in these substances is connected with the existence and dynamics of very strong hydrogen bonds between the carboxyls of the amino acid ions.

Among the members of this group that are so far known, the addition compounds of glycine predominate over other amino acids. For example, for the third simplest α-amino acid, valine, until recently the crystal structure of only one compound was known, DL-valine nitrate ($P2_1/c$, $a = 9.570(5)$, $b = 5.600(3)$, $c = 16.646(7)$ Å, $\beta = 105.19(6)^\circ$, $Z = 4$, $R = 0.12$) (4). In 1997, the structure of an analogous compound of L-valine, called bis(L-valine nitrate) ($P2_1$, $a = 5.635(2)$, $b = 18.478(3)$, $c = 8.504(4)$ Å, $\beta = 98.2079^\circ$, V = 876.4(5) Å^3, $Z = 2$, $R = 0.068$) was published (5).

The submitted work, which is part of our project dealing with selected H-bonded solids with potentially ferroelectric or proton conducting properties, is devoted to the study of mono-L-valinium nitrate (MVN)—the only addition compound found in the L-valine–nitric acid–water system. In addition to new and more precise solving of the crystal structures at different temperatures, the vibrational spectra of MVN and of its deuterated and ^{15}N-substituted analogs have been measured and interpreted. FTIR measurements down to low temperatures and DSC measurements in a broad temperature interval were carried out to study structural phase transition.

EXPERIMENTAL

Crystals of MVN were prepared by slow spontaneous evaporation of L-valine (99%, Aldrich) solution in nitric acid (p.a., Lachema, 1 mol L^{-1}) (in a molar ratio of 1:1) at laboratory temperature. The colorless crystals obtained were collected under vacuum on an S3 frit, washed with ethanol, and dried in the air. The ^{15}N-substituted (HNO_3) analog was similarly prepared from a solution containing $H^{15}NO_3$ (98% ^{15}N, Aldrich) by crystallization in a desiccator over KOH. The deuterated compound ($(CH_3)_2CHND_3^+CHCOOD.NO_3^-$) was prepared by repeated recrystallization of natural MVN from D_2O (99%) in a desiccator over KOH.

[1]To whom correspondence should be addressed. Fax: +420 2 21952378. E-mail: agnemec@natur.cuni.cz.

0022-4596/01 $35.00

TABLE 1
Basic Crystallographic Data, Data Collection, and Refinement Parameters for MVN

Temperature	293 K (phase I)	130 K (phase II)
Empirical formula	$C_5H_{12}N_2O_5$	
a	10.8369(3) Å	10.765(2) Å
b	18.4590(10) Å	18.2290(10) Å
c	5.62190(2) Å	11.109(2) Å
β	129.07(3)°	128.64(1)°
V	873.11(5) Å^3	1702.7(5) Å^3
Z	4	8
D (calc)	1.371 Mg m^{-3}	1.406 Mg m^{-3}
Crystal system	Monoclinic	
Space group	$P2_1$	
M_r	180.17	
μ(Mo$K\alpha$)	0.122 mm^{-1}	0.125 mm^{-1}
F(000)	384	768
Crystal dimensions	$0.14 \times 0.2 \times 0.5$ mm	
Diffractometer and radiation used	Enraf-Nonius CAD4-MACH III, Mo$K\alpha$, $\lambda = 0.71073$ Å	
Scan technique	θ–2θ	
No. and θ range of reflections for lattice parameter refinement	25, 15 → 16	
Range of h, k, and l	$-13 \rightarrow 10$, $0 \rightarrow 23$, $0 \rightarrow 7$	$0 \rightarrow 14$, $0 \rightarrow 24$, $-15 \rightarrow 11$
No. of standard reflections	3	3
Standard reflections monitored in interval	60 min	60 min
Intensity variation	3%	2.5%
Total No. of reflections measured:	2134	4860
θ Range	2.21–26.96°	2.07–28.97°
No. of independent reflections (R_{int})	1954 (0.0122)	4645 (0.0175)
No. of observed reflections	1514	4316
Criterion for observed reflections	$I > 2\sigma(I)$	
Absorption correction	None	
Function minimized	$\sum w(F_o^2 - F_c^2)^2$	
Weighting scheme	$w = [\sigma^2(F_o^2) + (0.1019P)^2 + 0.08P]^{-1}$	$w = [\sigma^2(F_o^2) + (0.0476P)^2 + 0.10P]^{-1}$
	$P = (F_o^2 + 2F_c^2)/3$	
Parameters refined	294	626
Value of R	0.0509	0.0257
Value of wR	0.1373	0.0686
Value of S	1.120	1.066
Extinction coefficient	0.041(9)	0.0108(10)
Max. and min. heights in final $\Delta\rho$ map	0.276, −0.168 e Å^{-3}	0.401, −0.221 e Å^{-3}
Source of atomic scattering factors	SHELXL 97(18)	
Programs used	SHELXL 97(18), PARST (19), PLUTO (20)	

The contents of carbon (theoretical content 33.33%, found 33.6%), nitrogen (theoretical content 15.55%, found 15.3%), and hydrogen (theoretical content 6.73%, found 6.7%) were determined using a Perkin–Elmer 240 C elemental analyzer.

The infrared spectra of nujol and fluorolube mulls were recorded on a Mattson Genesis FTIR spectrometer (2 cm^{-1} resolution, Beer–Norton medium apodization) in the 400–4000 cm^{-1} region. Low-temperature measurements were carried out by the nujol mull method in low-temperature cell with KBr windows in the 298–90 K interval. The temperature was controlled by a Fe–Const. thermocouple. The analog signal was processed on a PC using the AX5232 temperature measurement board.

The Raman spectra of polycrystalline samples were recorded on a Bruker RFS 100 FT Raman spectrometer (2 cm^{-1} resolution, Blackman-Harris 4-Term apodization, 1064 nm NdYAG laser excitation, 200 mW power at the sample) in the 50–4000 cm^{-1} region.

The DSC measurements were carried out on a Perkin Elmer DSC 7 power-compensated apparatus in the 95–400 K temperature region (helium or nitrogen atmosphere). A heating rate of 10 K min^{-1} was selected to measure approximately 10 mg of finely ground sample placed in an aluminum capsule.

The X-ray data collections for the MVN single crystal were carried out on an Enraf-Nonius CAD4-MACH III four-circle diffractometer (Mo$K\alpha$, graphite monochromator).

TABLE 2
Selected Bond Lengths (Å) and Angles (°) for MVN—Phase I

Bond	Value	Angle	Value	Angle	Value
N(1)–O(120)	1.214(4)	O(120)–N(1)–O(110)	122.2(3)	H(111)–N(11)–H(112)	117(6)
N(1)–O(110)	1.244(4)	O(120)–N(1)–O(130)	120.5(3)	H(111)–N(11)–H(113)	110(7)
N(1)–O(130)	1.273(4)	O(110)–N(1)–O(130)	117.3(3)	H(112)–N(11)–H(113)	101(6)
N(2)–O(230)	1.221(5)	O(230)–N(2)–O(210)	120.6(4)	O(22)–C(21)–O(21)	125.8(3)
N(2)–O(210)	1.246(5)	O(230)–N(2)–O(220)	122.6(4)	O(22)–C(21)–C(22)	123.0(4)
N(2)–O(220)	1.250(5)	O(210)–N(2)–O(220)	116.8(3)	O(21)–C(21)–C(22)	111.2(3)
C(11)–O(12)	1.199(5)	O(12)–C(11)–O(11)	126.5(4)	N(21)–C(22)–C(21)	108.4(3)
C(11)–O(11)	1.311(5)	O(12)–C(11)–C(12)	123.2(4)	N(21)–C(22)–C(23)	110.5(4)
C(11)–C(12)	1.511(5)	O(11)–C(11)–C(12)	110.3(4)	C(21)–C(22)–C(23)	113.3(4)
C(12)–N(11)	1.481(5)	N(11)–C(12)–C(11)	109.2(3)	C(25)–C(23)–C(252)	91(1)
C(12)–C(13)	1.554(7)	N(11)–C(12)–C(13)	113.4(4)	C(25)–C(23)–C(22)	118.9(8)
C(13)–C(142)	1.31(1)	C(11)–C(12)–C(13)	109.1(4)	C(252)–C(23)–C(22)	120.3(9)
C(13)–C(14)	1.41(1)	C(142)–C(13)–C(14)	93(1)	C(25)–C(23)–C(24)	90(2)
C(13)–C(152)	1.52(3)	C(142)–C(13)–C(152)	124(1)	C(252)–C(23)–C(24)	113(2)
C(13)–C(15)	1.56(2)	C(14)–C(13)–C(152)	99(1)	C(22)–C(23)–C(24)	116(1)
C(21)–O(22)	1.202(5)	C(142)–C(13)–C(12)	113.0(8)	C(25)–C(23)–C(242)	118.4(9)
C(21)–O(21)	1.299(5)	C(14)–C(13)–C(12)	120.0(7)	C(252)–C(23)–C(242)	107(1)
C(21)–C(22)	1.510(5)	C(152)–C(13)–C(12)	107(1)	C(22)–C(23)–C(242)	101.1(8)
C(22)–N(21)	1.487(5)	C(142)–C(13)–C(15)	99(1)	C(21)–O(21)–H(21)	120(8)
C(22)–C(23)	1.528(8)	C(14)–C(13)–C(15)	114(1)	C(22)–N(21)–H(211)	113(5)
C(23)–C(25)	1.39(2)	C(152)–C(13)–C(15)	27(1)	C(22)–N(21)–H(212)	110(4)
C(23)–C(252)	1.40(2)	C(12)–C(13)–C(15)	113.0(9)	C(22)–N(21)–H(213)	109(7)
C(23)–C(24)	1.55(3)	C(11)–O(11)–H(11)	111(6)	H(211)–N(21)–H(212)	105(7)
C(23)–C(242)	1.63(2)	C(12)–N(11)–H(111)	110(4)	H(211)–N(21)–H(213)	109(7)
		C(12)–N(11)–H(112)	114(5)	H(212)–N(21)–H(213)	112(7)
		C(12)–N(11)–H(113)	113(4)		

Hydrogen bonds

Donor–H		Donor ··· Acceptor		H ··· Acceptor		Donor–H ··· Acceptor	
O(11)–H(11)	0.70(12)	O(11) ··· O(130)^{i}	2.674(6)	H(11) ··· O(130)^{i}	2.02(11)	O(11)–H(11) ··· O(130)^{i}	156(7)
N(11)–H(111)	0.86(9)	N(11) ··· O(130)^{iii}	2.965(6)	H(111) ··· O(130)^{iii}	2.11(9)	N(11)–H(111) ··· O(130)^{iii}	178(4)
N(11)–H(112)	0.95(8)	N(11) ··· O(110)^{ii}	2.825(5)	H(112) ··· O(110)^{ii}	1.90(7)	N(11)–H(112) ··· O(110)^{ii}	163(5)
N(11)–H(113)	1.24(8)	N(11) ··· O(22)^{iv}	2.928(5)	H(113) ··· O(22)^{iv}	1.97(8)	N(11)–H(113) ··· O(22)^{iv}	131(5)
O(21)–H(21)	0.99(11)	O(21) ··· O(220)^{ii}	2.612(5)	H(21) ··· O(220)^{ii}	1.65(11)	O(21)–H(21) ··· O(220)^{ii}	161(8)
N(21)–H(211)	0.90(7)	N(21) ··· O(230)^{i}	3.171(6)	H(211) ··· O(230)^{i}	2.28(7)	N(21)–H(211) ··· O(230)^{i}	174(6)
N(21)–H(211)	0.90(7)	N(21) ··· O(210)^{i}	2.950(5)	H(211) ··· O(210)^{i}	2.40(8)	N(21)–H(211) ··· O(210)^{i}	120(6)
N(21)–H(212)	0.96(7)	N(21) ··· O(210)^{v}	2.900(6)	H(212) ··· O(210)^{v}	1.94(7)	N(21)–H(212) ··· O(210)^{v}	175(4)
N(21)–H(213)	0.93(9)	N(21) ··· O(12)^{iv}	2.888(6)	H(213) ··· O(12)^{iv}	2.16(12)	N(21)–H(213) ··· O(12)^{iv}	135(8)

Note. Equivalent positions: (i) $-x, y+\frac{1}{2}, -z-1$; (ii) $-x+1, y+\frac{1}{2}, -z+1$; (iii) $-x+1, y+\frac{1}{2}, -z$; (iv) $x, y, z-1$; (v) $-x, y+\frac{1}{2}, -z$.

The temperature of the crystal was controlled by an Oxford Cryosystems liquid nitrogen Cryostream Cooler. The phase problem was solved by direct methods and the nonhydrogen atoms were refined anisotropically, using the full-matrix least-squares procedure. The H atom positions were found from the difference Fourier map and their displacement factors were refined isotropically. The basic crystallographic data and the details of the measurement and refinement are summarized in Table 1. Crystallographic data for the MVN phases I and II have been deposited with the Cambridge Crystallographic Data Centre as Supplementary Publications CCDC-147849 and CCDC-147850, respectively. Copies of the data can be obtained free of charge on application to CCDC, 12 Union Road, Cambridge CB21EZ, UK (Fax: (+44) 1223-336-033; E-mail: deposit@ccdc.cam.ac.uk). A list of the observed and calculated structural factors is available from the authors upon request.

RESULTS AND DISCUSSION

The Crystal Structure of MVN

Bond lengths and angles of MVN phases I and II including those for the hydrogen bonds, are listed in Tables 2 and 3. The atom numbering of the both phases can be seen in Figs. 1 and 2. Packing schemes of valinium cations

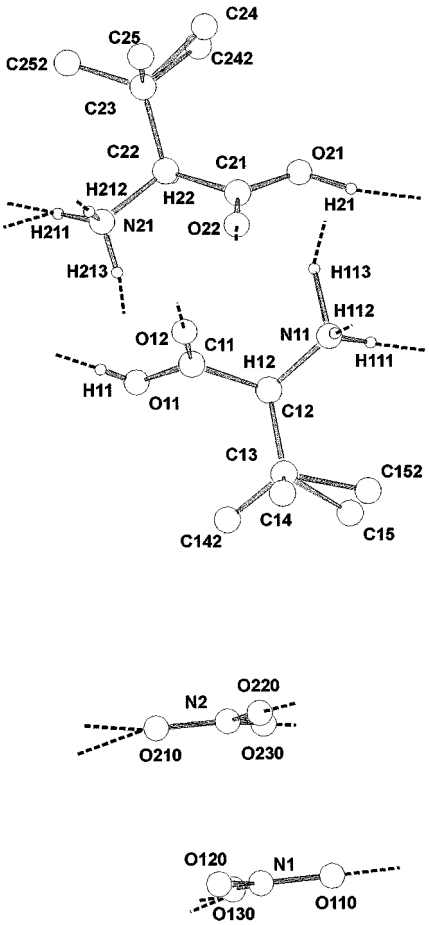

FIG. 1. Atom numbering in MVN phase I. Dashed lines indicate hydrogen bonds.

and nitrate anions of phases I and II are depicted in Figs. 3 and 4.

The crystal structures are formed by L-valinium cations ($(CH_3)_2CHNH_3^+CHCOOH$) and nitrate anions (NO_3^-) connected by an extensive system of hydrogen bonds (see Tables 2 and 3).

The asymmetric unit of phase I contains two valinium and two nitrates ions (see Fig. 1). This phase is characterized by the presence of methyl groups structural disorder between two positions (positions with 0.5 occupation factor C14, C142 and C15, C152 in the first valinium; C24, C242 and C25, C251 in the second one). No hydrogen atoms of isopropyl groups were localized due to this disorder at laboratory temperature.

Both carboxyl groups in MVN phase I are planar and only deviation (2.62 Å) of H11 atom from the plane is observed. The presence of valinium cations in the crystal structure is confirmed by corresponding increase of the C–O(H) bonds lengths (1.299 and 1.311 Å) compared to the C–O bonds (1.199 and 1.202 Å). The O–C–O(H) bonding angle values (125.8 and 126.5°) are slightly bigger than the corresponding angles in pure L-valine (124.8 and 124.9°) (6).

The bonding angles in the nitrate anions lie in the interval 116.8–122.6° and the bonding lengths have values from 1.214 to 1.273 Å. The reason for the deviations from the expected D_{3h} geometry apparently lies in the nonequivalent participation of the oxygen atoms of nitrate groups in the hydrogen bond system of the O–H ··· O and N–H ··· O types (see Table 2). Both nitrate groups are ideally planar with distortion of the atoms of the order of thousands of angstroms. The nitrate planes are almost parallel with interplane angle equal to 2.1°.

Low-temperature phase II exhibits an increase of the unit cell volume, by doubling the *c* axis value, and absence of isopropyl groups disorder (see Fig. 3). The asymmetric unit of this phase contains four valinium and four nitrate ions (see Fig. 2).

All carboxyl groups, including the hydrogen atoms, are planar and the maximum deviation from the carboxyl plane is that of atom H41, equal to 0.16 Å. The C–O(H) and C–O bonds lengths attain values of 1.308–1.318 Å and 1.207–1.215 Å, respectively. The O–C–O(H) bonding angle values lie in the 125.5–126.7° interval.

The bonding angles of the nitrate anions of MVN phase II lie in the interval 117.7–121.9° and the bonding lengths have values from 1.233 to 1.278 Å. All four nitrate groups are ideally planar with distortion of the atoms of the order of 0.001 Å. The nitrate planes are again almost parallel with interplane angle equal to 3.1–4.2°.

If these results are compared with the conclusions of Srinivasan *et al.* (5) for the same compound, called bis(L-valine nitrate) by these authors, the most obvious difference lies in the disorder of the isopropyl groups found for MVN at laboratory temperature. A similar disorder was not described for the crystal structure studied in their work, and the coordinates of all the hydrogen atoms were determined (unfortunately, without specification of the method used); however, the *R*-factor value obtained was worse (0.068 compared to 0.0509 in our work). Certain differences were also found in the bonding distances of the carbon atoms where, in addition to understandable differences for the isopropyl groups, their work gives a somewhat shorter distance between C_α neighbors (1.503 Å). A further difference lies in the relation between the bonding lengths for nitrate anions and the system of hydrogen bonds. In the case of both MVN phases, the greater lengthening of the N–O bond can be correlated quite well with the participation of the oxygen atom in shorter hydrogen bonds or pairs of medium-length H-bonds. In contrast, this trend cannot be unambiguously observed in the results of Srinivasan *et al.* Differences also exist in the types of H bonds in which the nitrate anions participate—for both MVN phases, the nitrates always participate in one bond of the O ··· H–O type and several

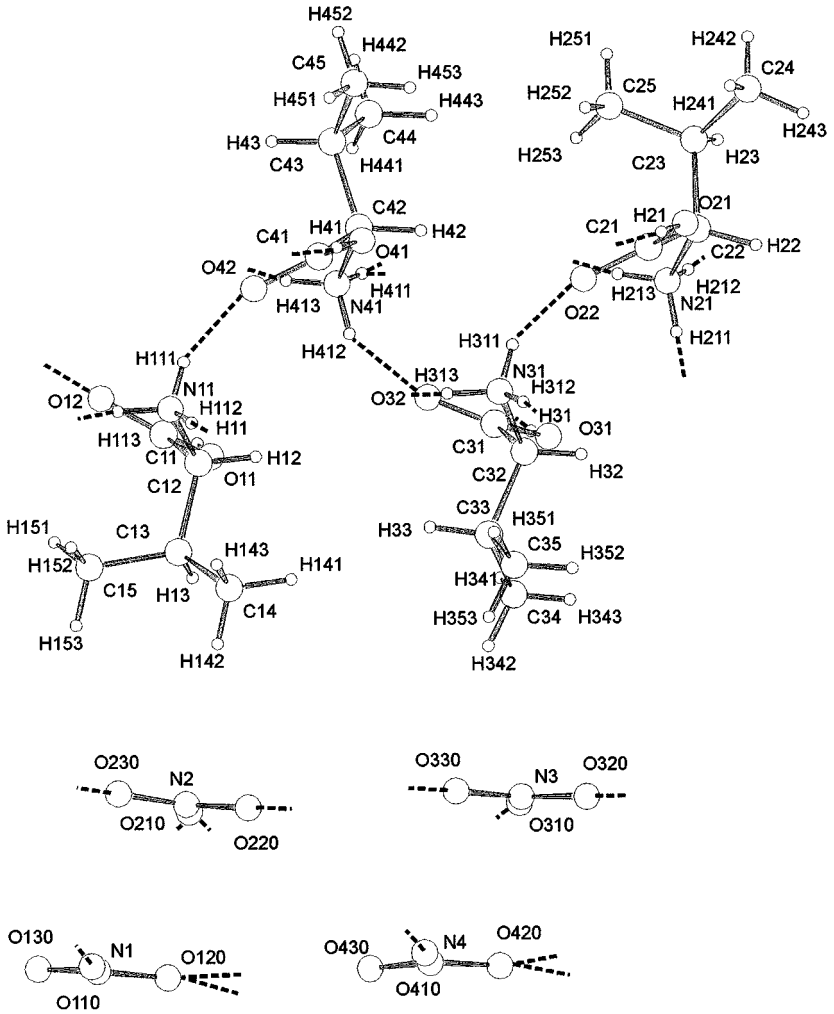

FIG. 2. Atom numbering in MVN phase II. Dashed lines indicate hydrogen bonds.

$O \cdots H-N$ bonds; however, in the work of Srinivasan and Rajaram, only hydrogen bonds of the $O \cdots H-N$ type can be expected for one of the pair of nitrates in the asymmetric unit.

Analysis of the Vibrational Spectra

The number of normal modes of the MVN crystal was determined by nuclear site group analysis (7). Standard correlation method (8) was used for more detailed study of the expected vibrational features of the nitrate group. The results obtained are presented in Tables 4 and 5. Both monoclinic MVN phases belong in the $P2_1$ (C_2^2) space group.

Crystals of phase I contain 48 atoms per asymmetric unit ($Z = 4$). All the atoms occupy two-fold positions $a(C_1)$. Four types of species present in the unit cell, two NO_3^- and two $(CH_3)_2CHNH_3^+CHCOOH$, occupying twofold positions $a(C_1)$, were considered in more detailed calculations of the internal and external modes.

Crystals of phase II contain 96 atoms per asymmetric unit ($Z = 8$). All the atoms once again occupy twofold positions $a(C_1)$. Eight types of species present in the unit cell, four nitrates, and four valinium cations, occupying twofold positions $a(C_1)$, were considered in more detailed calculations of the internal and external modes.

On the basis of nuclear site group analysis (see Table 4), it can be expected that the vibrational spectra of the MVN crystals will contain maximally twofold splitting of all the vibrational bands of each of the unit cell species. It is assumed that spectra of phase II could exhibit twice as many bands as phase I due to an increase of the unit cell species number. Such a level of splitting has not been observed in the obtained spectra, and, in addition, the total number of bands is much lower than the maximum number expected. These results could be explained by small interion interactions in

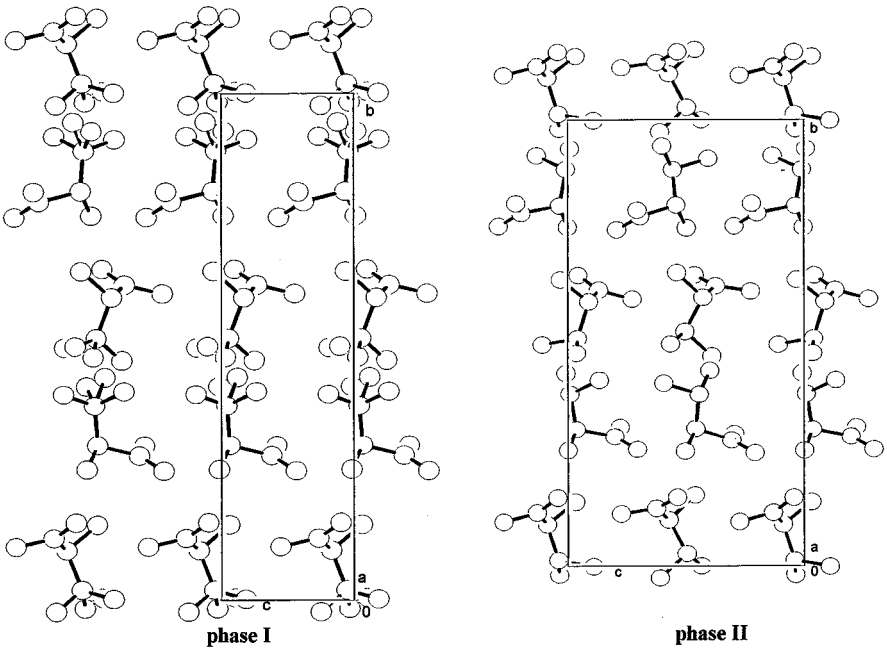

FIG. 3. Packing schemes of L-valinium cations in MVN phases. Hydrogen bonds are not projected.

the unit cell and also in terms of the fact that all the measurements were carried out on polycrystalline samples.

Vibrational Spectra of MVN

The IR spectra of MVN recorded at laboratory and low temperatures (90 K) are depicted in Fig. 5 together with the Raman spectrum; the peak positions are listed in Table 6. The IR and Raman spectra of deuterated MVN are depicted in Fig. 6 and the maxima are listed in Table 7. The overall character of the vibrational spectra is in accord with the results of MVN crystal structure determination, i.e., a compound consisting of L-valinium and nitrate ions, interconnected by a network of hydrogen bonds.

Assignment of the vibrational bands of MVN and its deuterate is based on the results of a previous study of the

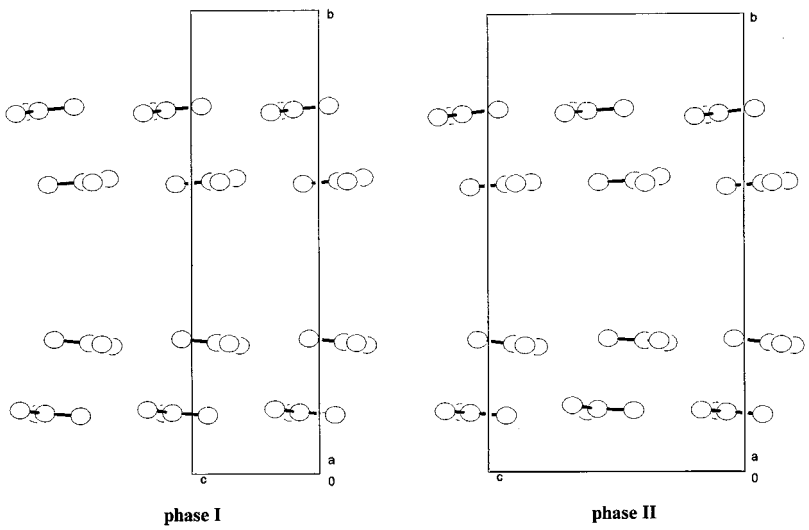

FIG. 4. Packing schemes of nitrate anions in MVN phases. Hydrogen bonds are not projected.

TABLE 3
Selected Bond Lengths (Å) and Angles (°) for MVN—Phase II

Bond	Value	Bond	Value	Angle	Value	Angle	Value
N(1)–O(130)	1.233(2)	C(21)–O(21)	1.308(2)	O(130)–N(1)–O(110)	121.6(1)	N(21)–C(22)–C(21)	107.9(1)
N(1)–O(110)	1.254(2)	C(21)–C(22)	1.516(2)	O(130)–N(1)–O(120)	120.8(1)	N(21)–C(22)–C(23)	110.6(1)
N(1)–O(120)	1.278(2)	C(22)–N(21)	1.491(2)	O(110)–N(1)–O(120)	117.7(1)	C(21)–C(22)–C(23)	113.4(1)
N(2)–O(220)	1.241(2)	C(22)–C(23)	1.544(2)	O(220)–N(2)–O(210)	120.2(1)	C(24)–C(23)–C(25)	111.6(1)
N(2)–O(210)	1.257(2)	C(23)–C(24)	1.524(2)	O(220)–N(2)–O(230)	121.8(1)	C(24)–C(23)–C(22)	111.1(1)
N(2)–O(230)	1.262(2)	C(23)–C(25)	1.531(2)	O(210)–N(2)–O(230)	118.0(1)	C(25)–C(23)–C(22)	112.9(1)
N(3)–O(320)	1.245(2)	C(31)–O(32)	1.213(2)	O(320)–N(3)–O(310)	119.7(1)	O(32)–C(31)–O(31)	126.7(1)
N(3)–O(310)	1.254(2)	C(31)–O(31)	1.316(2)	O(320)–N(3)–O(330)	121.9(1)	O(32)–C(31)–C(32)	122.0(1)
N(3)–O(330)	1.259(2)	C(31)–C(32)	1.520(2)	O(310)–N(3)–O(330)	118.3(1)	O(31)–C(31)–C(32)	111.2(1)
N(4)–O(430)	1.233(2)	N(31)–C(32)	1.491(2)	O(430)–N(4)–O(410)	121.3(1)	N(31)–C(32)–C(31)	108.7(1)
N(4)–O(410)	1.256(2)	C(32)–C(33)	1.538(2)	O(430)–N(4)–O(420)	121.0(1)	N(31)–C(32)–C(33)	111.1(1)
N(4)–O(420)	1.277(2)	C(33)–C(34)	1.523(2)	O(410)–N(4)–O(420)	117.7(1)	C(31)–C(32)–C(33)	109.0(1)
C(11)–O(12)	1.207(2)	C(33)–C(35)	1.525(2)	O(12)–C(11)–O(11)	126.6(1)	C(34)–C(33)–C(35)	110.0(1)
C(11)–O(11)	1.318(2)	C(41)–O(42)	1.215(2)	O(12)–C(11)–C(12)	123.8(1)	C(34)–C(33)–C(32)	110.2(1)
C(11)–C(12)	1.518(2)	C(41)–O(41)	1.313(2)	O(11)–C(11)–C(12)	109.6(1)	C(35)–C(33)–C(32)	111.9(1)
C(12)–N(11)	1.486(2)	C(41)–C(42)	1.518(2)	N(11)–C(12)–C(11)	109.1(1)	O(42)–C(41)–O(41)	125.6(1)
C(12)–C(13)	1.543(2)	C(42)–N(41)	1.489(2)	N(11)–C(12)–C(13)	113.7(1)	O(42)–C(41)–C(42)	122.4(1)
C(13)–C(15)	1.526(2)	C(42)–C(43)	1.545(2)	C(11)–C(12)–C(13)	110.2(1)	O(41)–C(41)–C(42)	111.9(1)
C(13)–C(14)	1.530(2)	C(43)–C(45)	1.519(2)	C(15)–C(13)–C(14)	111.9(1)	N(41)–C(42)–C(41)	107.7(1)
C(21)–O(22)	1.215(2)	C(43)–C(44)	1.520(2)	C(15)–C(13)–C(12)	113.7(1)	N(41)–C(42)–C(43)	110.1(1)
				C(14)–C(13)–C(12)	111.3(1)	C(41)–C(42)–C(43)	111.0(1)
				O(22)–C(21)–O(21)	125.5(1)	C(45)–C(43)–C(44)	109.4(1)
				O(22)–C(21)–C(22)	123.2(1)	C(45)–C(43)–C(42)	111.0(1)
				O(21)–C(21)–C(22)	111.3(1)	C(44)–C(43)–C(42)	111.1(1)

Hydrogen bonds

Donor–H		Donor ⋯ Acceptor		H ⋯ Acceptor		Donor–H ⋯ Acceptor	
O(11)–H(11)	0.78(4)	O(11) ⋯ O(420)^{i}	2.658(2)	H(11) ⋯ O(420)^{i}	1.90(4)	O(11)–H(11) ⋯ O(420)^{i}	164(2)
N(11)–H(111)	0.85(2)	N(11) ⋯ O(42)	2.915(2)	H(111) ⋯ O(42)	2.18(2)	N(11)–H(111) ⋯ O(42)	145(1)
N(11)–H(112)	0.84(3)	N(11) ⋯ O(120)^{ii}	2.955(2)	H(112) ⋯ O(120)^{ii}	2.14(3)	N(11)–H(112) ⋯ O(120)^{ii}	165(2)
N(11)–H(113)	0.88(3)	N(11) ⋯ O(410)^{i}	2.820(2)	H(113) ⋯ O(410)^{i}	1.95(3)	N(11)–H(113) ⋯ O(410)^{i}	166(2)
O(21)–H(21)	0.86(3)	O(21) ⋯ O(330)^{iii}	2.590(2)	H(21) ⋯ O(330)^{iii}	1.75(3)	O(21)–H(21) ⋯ O(330)^{iii}	165(3)
N(21)–H(211)	0.88(2)	N(21) ⋯ O(12)^{iv}	2.884(2)	H(211) ⋯ O(12)^{iv}	2.20(3)	N(21)–H(211) ⋯ O(12)^{iv}	135(2)
N(21)–H(212)	0.84(2)	N(21) ⋯ O(320)^{v}	3.083(2)	H(212) ⋯ O(320)^{v}	2.26(2)	N(21)–H(212) ⋯ O(320)^{v}	167(2)
N(21)–H(213)	0.86(3)	N(21) ⋯ O(210)^{i}	2.873(2)	H(213) ⋯ O(210)^{i}	2.02(3)	N(21)–H(213) ⋯ O(210)^{i}	172(2)
O(31)–H(31)	0.81(4)	O(31) ⋯ O(120)^{i}	2.668(2)	H(31) ⋯ O(120)^{i}	1.90(4)	O(31)–H(31) ⋯ O(120)^{i}	160(2)
N(31)–H(311)	0.86(2)	N(31) ⋯ O(22)	2.856(2)	H(311) ⋯ O(22)	2.10(2)	N(31)–H(311) ⋯ O(22)	146(1)
N(31)–H(312)	0.87(3)	N(31) ⋯ O(420)^{iii}	2.928(2)	H(312) ⋯ O(420)^{iii}	2.07(3)	N(31)–H(312) ⋯ O(420)^{iii}	171(2)
N(31)–H(313)	0.89(3)	N(31) ⋯ O(110)^{ii}	2.806(2)	H(313) ⋯ O(110)^{ii}	1.94(2)	N(31)–H(313) ⋯ O(110)^{ii}	165(2)
O(41)–H(41)	0.90(3)	O(41) ⋯ O(230)^{ii}	2.606(2)	H(41) ⋯ O(230)^{ii}	1.73(4)	O(41)–H(41) ⋯ O(230)^{ii}	164(3)
N(41)–H(411)	0.88(2)	N(41) ⋯ O(220)^{i}	3.231(2)	H(411) ⋯ O(220)^{i}	2.36(2)	N(41)–H(411) ⋯ O(220)^{i}	171(2)
N(41)–H(411)	0.88(2)	N(41) ⋯ O(210)^{i}	2.900(2)	H(411) ⋯ O(210)^{i}	2.37(2)	N(41)–H(411) ⋯ O(210)^{i}	119(2)
N(41)–H(412)	0.88(2)	N(41) ⋯ O(32)	2.814(2)	H(412) ⋯ O(32)	2.08(3)	N(41)–H(412) ⋯ O(32)	140(2)
N(41)–H(413)	0.87(3)	N(41) ⋯ O(310)^{i}	2.847(2)	H(413) ⋯ O(310)^{i}	1.99(3)	N(41)–H(413) ⋯ O(310)^{i}	172(2)

Note. Equivalent positions: (i) $-x, y+\frac{1}{2}, -z+1$; (ii) $-x+1, y+\frac{1}{2}, -z+2$; (iii) $-x+1, y+\frac{1}{2}, -z+1$; (iv) $x, y, z-1$; (v) $-x, y+\frac{1}{2}, -z$.

vibrational spectra of L-valine (9–13), nitrate (14), and the addition compounds of amino acids (15).

The stretching vibrations of the N–H and O–H groups interconnected by a system of hydrogen bonds in a crystal appear in the IR spectrum as broad, medium-intensity bands in the 3250–2350 cm^{-1} region (2400–2050 cm^{-1} region in the deuterate). It is apparent from the crystal structure (Tables 2 and 3) that these are hydrogen bonds of the N–H ⋯ O type with a length of 2.82–3.23 Å and of the O–H ⋯ O type with a length of 2.59–2.67 Å. On the basis of correlation curves (16, 17) between the wavenumbers of the *v*O–H or *v*N–H vibrations and the length of the hydrogen bonds, bands corresponding to the O–H ⋯ O and N–H ⋯ O bonds can be expected at 2600–3100 and 3000–3400 cm^{-1} regions, respectively. Temperature-sensitive band of out-of-plane O–H ⋯ O bending vibration,

TABLE 4
Results of the Nuclear Site Group Analysis for MVN

	Phase I		Phase II	
C_2^2	A	B	A	B
External modes				
Acoustical	1	2	1	2
Translational	11	10	23	22
Librational	12	12	24	24
Internal modes	120	120	240	240
Total	144	144	288	288
Activity				
IR	z	x, y	z	x, y
Raman	$\alpha_{xx}, \alpha_{yy}, \alpha_{zz}, \alpha_{xy}$	α_{yz}, α_{xz}	$\alpha_{xx}, \alpha_{yy}, \alpha_{zz}, \alpha_{xy}$	α_{yz}, α_{xz}

characteristic for this type of intermediate hydrogen bond, is located at ca. 870 cm^{-1}.

The stretching vibration of the CH and CH_3 groups can be observed in the 3000–2885 cm^{-1} region. These vibrations, which are quite intense in the Raman spectra, are almost masked in the IR spectra of natural MVN by the broad bands of the stretching N–H and O–H vibrations.

The area in vibrational spectra above 1800 cm^{-1} is expected to exhibit the overtone and combination bands of the fundamental vibrations.

The C=O stretching vibrations, indicating the presence of the valinium cations, are manifested in a band at 1715–1725 cm^{-1}. The existence of shoulders and observed splitting of this band (deuterated MVN) is in accord with the results of nuclear site group analysis (Table 4) and with the presence of structurally nonequivalent valinium ions in the unit cell. However, shoulder at 1755 cm^{-1} in the low-temperature IR spectrum could also be assigned to combination vibration of nitrate v_1 and v_4 modes.

The deformation vibrations of the NH_3^+ group were recorded in the 1620 to 1513 cm^{-1} region. The corresponding bands of the δ ND_3^+ vibrations were observed in the 1170–1130 cm^{-1} region in the spectra of deuterated compound.

The presence of L-valinium ions in the crystal structure is also reflected in the occurrence of highly mixed bands of the C–O stretching vibration (ca. 1380 cm^{-1}) and C–O–H in-plane bending vibration (ca. 1215 cm^{-1}), together with C–O–H out-of-plane bending vibration (809 cm^{-1}).

The expected manifold multiplication and splitting of all the nitrate internal vibration bands (see Table 5) was only partially observed for the originally doubly degenerate vibrations v_3 (doublet) and v_4 (doublet to triplet). Splitting of the fully symmetric v_1 vibration into two components has also been recorded even in the laboratory-temperature spectra. In order to confirm the interpretation of the NO_3^- internal vibrations, the spectra of the isotope-substituted compound $(CH_3)_2CHNH_3^+CHCOOH \cdot {}^{15}NO_3^-$ has been studied. Shifts were observed in the bands of both branches of the v_3 vibration by 28 cm^{-1} toward lower wavenumbers and of the band of the v_2 vibration by 22 cm^{-1} in the same direction. The positions and character of the bands of the v_1

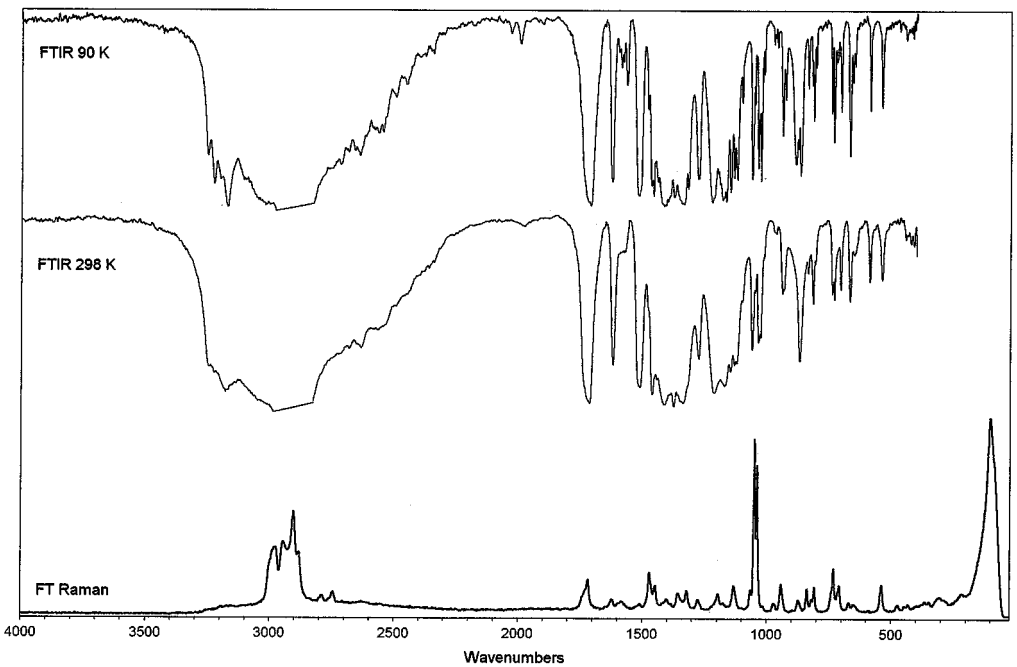

FIG. 5. FTIR (nujol mull) and FT Raman spectra of MVN.

TABLE 5
Correlation Analysis of NO_3^- Internal Modes in MVN Crystal

Free ion modes	Degree of freedom		Free ion symmetry	Site symmetry	Factor group symmetry	Vibration modes		Activity	
	Phase I	Phase II	D_{3h}	C_1	C_2	Phase I	Phase II	IR	Raman
ν_1	4	8	A_1'			$2\nu_1, 2\nu_2,$ $4\nu_3, 4\nu_4$	$4\nu_1, 4\nu_2,$ $8\nu_3, 8\nu_4$	z	α_{xx}, α_{yy} α_{zz}, α_{xy}
					A				
ν_2	4	8	A_2''	A					
ν_3	4	8	E'						
					B	$2\nu_1, 2\nu_2,$ $4\nu_3, 4\nu_4$	$4\nu_1, 4\nu_2,$ $8\nu_3, 8\nu_4$	$x,$ y	α_{yz}, α_{xz}
ν_4	4	8	E'						

and ν_4 vibrations and of all the vibrational bands of L-valinium remained unchanged.

In the Raman spectra of the natural and deuterated compounds, the external modes are located in the region below 100 cm^{-1}.

Thermal Behavior of MVN

Crystals of MVN are stable in the air up to a temperature of 402 K, where they melt. The natural and deuterated compounds were further studied by the DSC method from a temperature of 95 K up to 400 K. The only phase transition between the phases I and II was found at low temperature ($\Delta H = 200.0$ J mol^{-1}, heating onset 249 K, cooling onset 248 K) (see Fig. 7). The phase transition is very likely to be of the first-order type (according to peak shape). The fact that the parameters of this transition are not practically affected by deuteration of the compound ($\Delta H = 250.4$ J mol^{-1}, heating onset 250 K) (see Fig. 7) confirms X-ray structure determination results that the phase transition mechanism is not affected by the H-bonds network.

The FTIR spectra (see Figs. 5, 8; Table 6) were recorded in the temperature interval 298–90 K. The expected increase

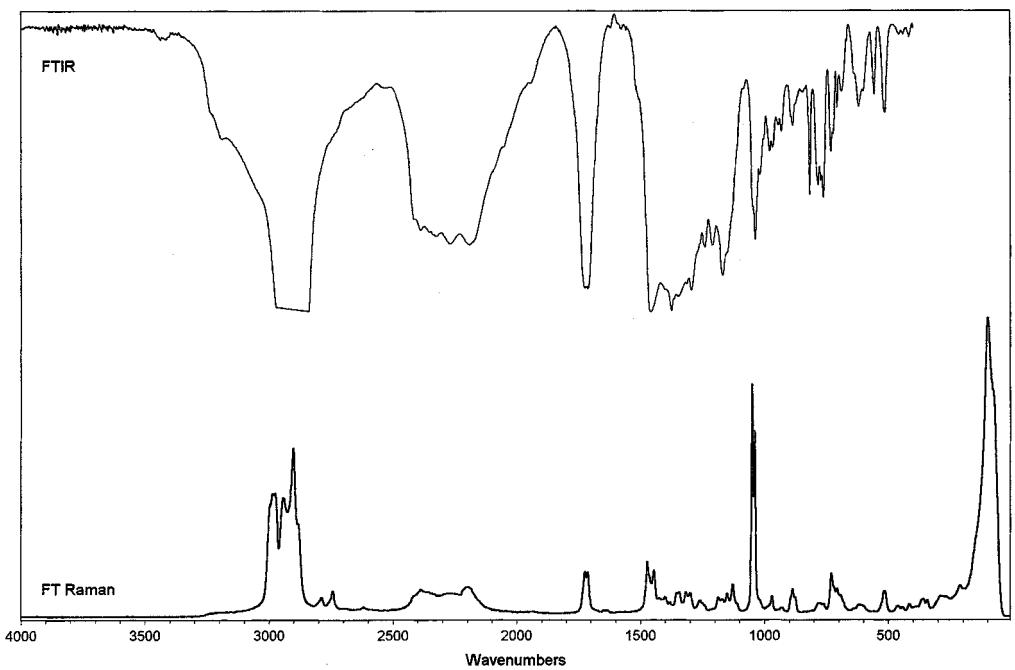

FIG. 6. FTIR (nujol mull) and FT Raman spectra of deuterated MVN.

TABLE 6
FTIR and FT Raman Spectra of MVN

Assignment	IR 298 K	IR 90 K	Raman (peak intensity)	Assignment	IR 298 K	IR 90 K	Raman (peak intensity)
νN–H ⋯ O, νO–H ⋯ O	3250 sh	3253 m		ρCH_3		1201 m	
		3227 m				1193 s	1195(10)
		3202 m			1183 sh	1183 s	
	3181 s	3173 s	3175(4)		1173 s	1178 sb	1175(5)
	3050 s				1168 s	1169 s	
$\nu_{as}CH_3$			3000 sh		1149 m	1151 s	
			2990 sh		1133 m	1136 m	1132(14)
$\nu C_\alpha H$	2972 s	n.o.[a]	2975(34)		1124 m	1124 n	
νCH	2940 s	n.o.[a]	2946(37)		1102 w	1104 w	
$\nu_s CH_3$			2904(52)	ρNH_3^+	1062 m	1064 m	1065(12)
?	2885 sh	n.o.[a]	2883(32)			1054 w	
νN–H ⋯ O, νO–H ⋯ O		2760 mb	2788(10)	ν_1 NO_3^-	1050 w	1048 w	1050(88)
	2719 m	2720 m	2745(12)		1037 m	1040 m	1040(75)
	2683 m	2690 m		ρNH_3^+, νCC, νCN		1035 m	
		2662 m			1028 m	1028 m	
	2636 m	2642 m	2630(7)	νCC, νCN	1015 w	1015 w	1015(4)
	2568 m	2566 m				976 w	
		2548 m			970 wb	971 w	972(5)
?		2497 w				962 w	
		2456 w		ρNH_3^+, νCC, νCN	940 w	941 m	942(14)
		2379 w			934 w	930 w	
		2347 w		γO–H ⋯ O, νCC, νCN		889 m	
		2034 w				878 m	
νC=O	1979 w	1995 w			871 m	870 m	874(6)
		1755 sh					
	1735 sh	1721 sh	1730 sh	ρNH_3^+	838 w	839 w	838(12)
						823 w	
	1715 s	1712 s	1719(17)	$\nu_2 NO_3^-$	818 w	817 m	819(7)
$\delta_{as}NH_3^+$	1621 m	1626 m	1622(7)	γC–O–H	809 w	808 w	809(13)
		1600 w		$\nu_4 NO_3^-$	741 w	745 m	
		1590 w			732 w	735 m	732(22)
	1585 wb	1582 w	1585(6)			725 w	
		1568 w		ωCOO		714 w	
$\delta_s NH_3^+$		1523 s			707 w	706 w	709(14)
	1518 s	1519 s	1510(5)			675 sh	
	1513 s	1513 sh			669 w	671 m	670(5)
$\delta_{as}CH_3$	1480 sh	1483 w				660 w	
	1466 m	1468 s	1472(21)		652 w	651 w	653(4)
	1444 m	1443 m	1448(14)	ρCOO	590 w	590 w	592(1)
?		1425 sh			540 w	542 w	538(14)
$\nu_3 NO_3^-$	1416 s	1418 s		δ Skelet.	473 w	471 w	474(4)
δ_s CH_3		1410 s			445 w	445 w	448(3)
		1402 s	1402(7)		424 w	417 w	432(4)
	1394 s	1394 s			412 w		
νC–O	1382 s	n.o.[a]	1383(5)				365(6)
$\delta C_\alpha H$	1363 s		1357(10)				349(6)
	1351 sh	1354 s		τCH_3			306(9)
		1345 s		γCH			214(11)
$\nu_3 NO_3^-$	1339 s	1338 s		External mode			103(100)
$\delta_s CH_3$	1320 sh	1321 s	1321(11)				
δCH		1281 m					
	1277 m	1277 m	1277(7)				
δC–O–H, δCH		1225 s					
	1214 s	1218 s					

[a]Not observed due to nujol bands.

Note. vs, very strong; s, strong; m, medium; w, weak; b, broad; sh, shoulder; ν, stretching; δ, deformation or in-plane bending; τ, torsional; γ, out-of-plane bending; ρ, rocking; ω, wagging; $_s$, symmetric; $_{as}$, antisymmetric.

TABLE 7
FTIR and FT Raman Spectra of Deuterated MVN

Assignment	IR	Raman (peak intensity)	Assignment	IR	Raman (peak intensity)
$2\nu C{=}O$	3430 w		$\nu_1\ NO_3^-$	1049 sh	1050(81)
?	3190 w	3200(2)		1038 m	1041(64)
	3040 sh		νCC, νCN	1018 w	1020 sh
$\nu_{as}CH_3$		2988(42)		1003 w	
$\nu C_\alpha H$	2973 m	2978(42)		980 w	
νCH	2941 m	2944(4)		968 w	970(7)
$\nu_s CH_3$	2905 m	2904(57)		945 w	
?	2883 m	2884(31)		933 w	930(3)
		2789(7)		895 sh	
	2770 sh	2744(9)	νCC, νCN, $\delta C{-}O{-}D$	887 w	888(9)
		2619(3)		875 sh	877(7)
$\nu N{-}D\cdots O$, $\nu O{-}D\cdots O$	2420 m	2420(7)	?	845 wb	
	2390 m	2385(9)	$\nu_2 NO_3^-$	818 m	
	2335 m		ρND_3^+	784 w	784(5)
	2272 m	2275(8)		773 w	
	2192 m	2200(10)		763 m	762(4)
?	1945 w		$\nu_4 NO_3^-$	733 w	731(15)
$\nu C{=}O$	1726 s	1725(15)		725 w	
	1715 s	1714(15)	ωCOO	708 w	708(9)
?		1648(2)		690 w	
		1636(2)	ωCOO, γODO, ρND_3^+	640 sh	
$\delta_{as}CH_3$	1465 m	1474(19)		620 w	618(4)
		1447(15)		603 w	
$\nu_3 NO_3^-$, $\delta_s CH_3$		1425(6)	ρCOO	557 w	
	1403 s	1402(7)		515 w	517(8)
$\nu C{-}O$	1386 s	1383(5)	δ Skelet.	459 w	463(4)
$\delta C_\alpha H$	1365 s	1356(8)		442 w	444(3)
$\nu_3\ NO_3^-$	1349 s	1345(8)		418 w	417(4)
$\delta_s CH_3$	1315 s	1318(8)			360(6)
δCH	1297 s	1300(8)			345(5)
	1241 m	1260(6)	τCH_3		285(7)
	1212 m		γCH		213(10)
ρCH_3, $\delta_{as}ND_3^+$		1187(6)	External modes		101(100)
	1170 s	1170(6)			79 sh
ρCH_3, $\delta_s ND_3^+$	1155 sh	1152(8)			
		1129(11)			

Note. Abbreviations as for Table 6.

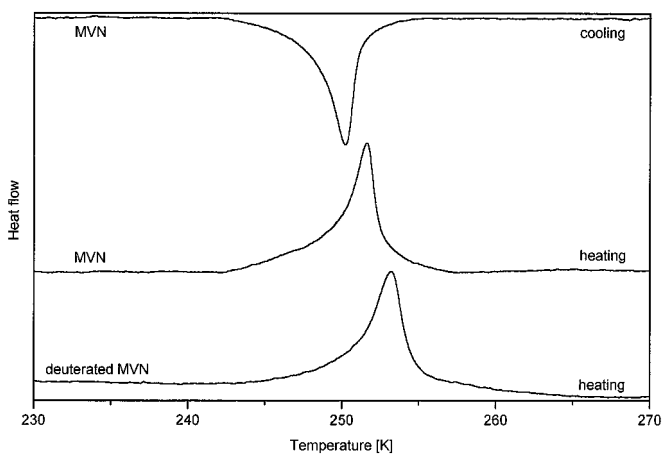

FIG. 7. DSC curves of MVN.

of the vibrational bands number in the MVN phase II spectra (due to increase of Z) was partially observed only for some types of vibrations (i.e., $\delta\ NH_3^+$, $\delta_s CH_3$, ρCH_3, νCC, νCN, etc.). However, in general, the minimal changes in the spectra observed on a decrease in the temperature are in agreement with the phase transition mechanism based mainly on ordering of the methyl groups, i.e., without structural changes related to the polar groups and thus the system of hydrogen bonds.

Both MVN phases match a necessary symmetry condition (polar crystallographic class 2) for ferroelectric materials; however, the facts that no phase transition from ferroelectric to paraelectric phase was observed and that in crystal structure there is not present any strong $O{-}H\cdots O$ hydrogen bond connecting carboxyls, which is characteristic for the TGS family of ferroelectrics, lead to the

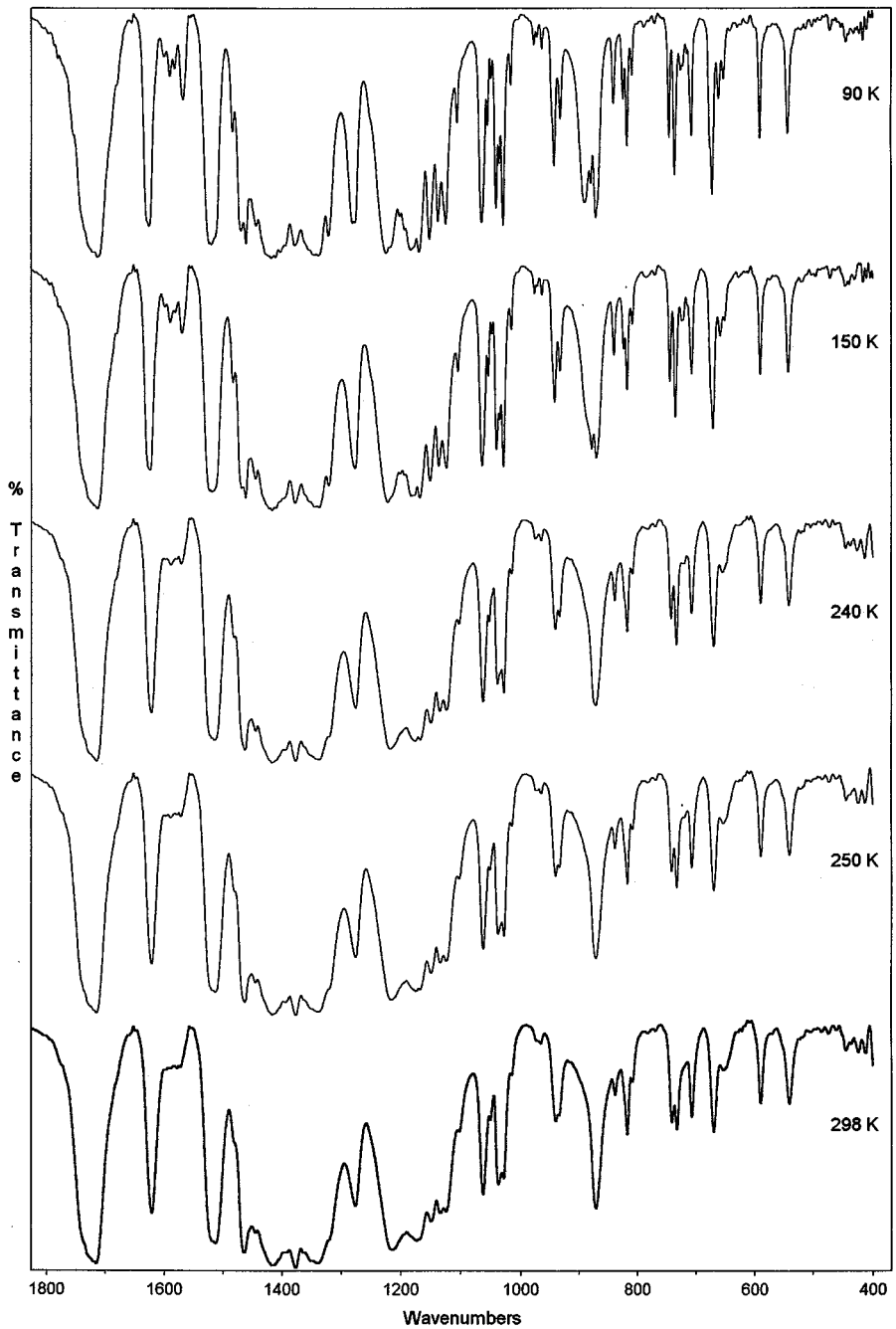

FIG. 8. FTIR spectra (nujol mull) of MVN at different temperatures.

conclusion that the possibility of ferroelectric properties existence for MVN crystals is minimal. Research of MVN will continue with measurements of dielectric properties.

ACKNOWLEDGMENTS

This study was carried out with financial assistance from the Grant Agency of the Czech Republic, Grant 203/98/1198, and the Grant Agency of Charles University of Prague, Grant 13/1998/B CH.

REFERENCES

1. M. I. Kay and R. Kleinberg, *Ferroelectrics* **5,** 45 (1973).
2. S. Sato, *J. Phys. Soc. Jpn.* **25,** 185 (1968).
3. M. Ichikawa, *Ferroelectrics* **39,** 1033 (1981).
4. S. N. Rao and R. Parthasarathy, *A. C. A.* (Spring) 129 (1974).
5. N. Srinivasan, P. K. Rajaram, and D. D. JebaRaj, *Z. Kristallogr.* **212**(4), 313 (1997).
6. K. Torii and Y. Iitaka, *Acta Crystallogr. B* **26,** 1317 (1970).
7. D. L. Rousseau, R. P. Bauman, and S. P. S. Porto, *J. Raman Spectrosc.* **10,** 253 (1981).

8. W. G. Fateley, N. T. McDevit, and F. F. Bentley, *Appl. Spectrosc.* **25,** 155 (1971).
9. U. Stahlberg and E. Steger, *Spectrochem. Acta A* **23,** 475 (1967).
10. A. R. Gargaro, L. D. Barron, and L. Hecht, *J. Raman Spectrosc.* **24,** 91 (1993).
11. A. Pawlukojc, L. Bobrowicz, and I. Natkaniec, *Spectrochem. Acta A* **51,** 303 (1995).
12. L. A. Nafie, M. R. Oboodi, and T. B. Freedman, *J. Am. Chem. Soc.* **105,** 7449 (1983).
13. L. Burman, P. Tandon, V. D. Gupta, and S. Rastogi, *Polym. J.* **28**(6), 474 (1996).
14. K. Nakamoto, *in* "Infrared and Raman Spectra of Inorganic and Coordination Compounds," 4th ed, p. 124. Wiley, New York, 1986.
15. M. Tsuboi, T. Takenishi, and A. Nakamura, *Spectrochem. Acta* **19,** 271 (1963).
16. A. Novak, *Struct. Bonding* **18,** 177 (1974).
17. A. Lautie, F. Froment, and A. Novak, *Spectrosc. Lett.* **9**(5), 289 (1976).
18. G. M. Sheldrick, SHELXL 97, University of Göttingen, 1997.
19. H. Nardelli, "PARST, A System for Computer Routines for Calculating Molecular Parameters from Results of Crystal Structure Analysis." University of Parma, 1982.
20. R. Brueggeman and G. Schmid, PLUTO v. 5.13. University of Ulm, 1993.